Observation of nanosize effect in lateral nanoscale *p-n* and *p-i-n* junctions

Arief Udhiarto, Sri Purwiyanti
Electrical Engineering Department, Faculty of Engineering
Universitas Indonesia
Depok, Indonesia
arief.udhiarto@ui.ac.id

Daniel Moraru, Takeshi Mizuno, Michiharu Tabe
Research Institute of Electronics
Shizuoka University, 3-5-1 Johoku, Naka-ku,
Hamamatsu, 432-8011, Japan

***Abstract*— We study nanosize-effect in lateral nanoscale *p-n* and *p-i-n* junction devices under light illumination. Current versus voltage (*I-V*) and current versus time (*I-time*) characteristics were investigated at low and at room temperature. At low temperature, only *p-n* junction devices show a photon sensitivity in *I-V* characteristics due to co-existence of donor-acceptor pair. At room temperature, both devices show photovoltaic nature, i.e., increase of reverse current is observed under light illumination. In addition, devices with narrow channel-width tend to produce larger photocurrent which is ascribed to the nanosize effect.**

***Keywords*— Nanoscale p-n and p-i-n junctions; individual dopants; nanosize effect**

I. Introduction

Silicon based *p-i-n* and *p-n* devices have been commonly used for a variety of photonic and electronic applications along with semiconductor history [1]. Taking advantages of present fabrication technology, recently, novel properties of nanoscale *p-i-n* and *p-n* junctions have been studied and their advantages have been demonstrated [2–7]. Co-axial *p-i-n* and *p-n* nanowires are reported to be highly efficient in solar cell applications [2,3]. Two-dimensional (2D) *p-n* junctions are known to have a higher breakdown voltage and a lower capacitance than conventional *p-n* junctions [6]. Also, 2D *p-n* junctions have enhanced photoluminescence and electroluminescence efficiency, because of quantum-mechanical confinement effect of carriers [7]. Thus, nanoscale *p-i-n* and *p-n* diodes are of increasing importance for novel photodevices.

It is important to be noted that as devices are scaled down into nanometer scale, the number of dopant atoms is limited and countable. In this nanoscale regime, individual dopant atom potential may influence the device operation. In fact, nanoscale MOSFETs with doped-channels have been intensively studied [8–15]. In those single-dopant devices, individual potentials of dopant atoms are intentionally utilized as miniaturized quantum dots. The role of individual dopant atoms in nanoscale lateral *p-n* junctions at low temperature has also been reported [16]. Since room temperature operation is the main goal for more practical application, it is important to study room temperature behavior of nanoscale lateral *p-n* and *p-i-n* junctions and their characteristics under light illumination. The effects of nanosize also need to be clarified.

In this work, we first present a review of low temperature characteristics of nanoscale lateral *p-n* and *p-i-n* junction devices. Next, we study room temperature characteristics and the effect of channel width. The devices are characterized in dark and under light illumination. As a result, at low temperature, only *p-n* junction devices show a photon sensitivity in *I-V* characteristics which is ascribed to the charging and discharging of donor-acceptor pair by photogenerated carrier. At room temperature, we found that both *p-n* and *p-i-n* devices show photovoltaic nature, i.e., current is enhanced in the reverse bias condition under light illumination. It is even more important that, narrow channel-width devices show higher photo response and it is ascribed to the nanosize effects.

II. Methodology

We fabricated and studied two types of nanoscale diode, *p-n* and *p-i-n*. Schematic device structure, bias configuration and schematic top view for both devices are shown in Fig. 1. The nanodiode was patterned on silicon-on-insulator (SOI) structure using electron beam lithography. The width, length, and thickness are estimated to be 15, 1000, and 5 nm, respectively. Boron and phosphorus atoms were selectively diffused to create lateral *p-n* junction and *p-i-n* devices. In *p-n* junction devices, a co-doped region was doped with phosphorus and boron simultaneously. Boron concentration is higher than phosphorus concentration. For both devices, final phosphorous and boron concentration derived from secondary ion mass spectrometry (SIMS) are estimated to be $N_D \approx 1 \times 10^{18}$ cm^{-3} and $N_A \approx 1.5 \times 10^{18}$ cm^{-3} respectively. In the *p-i-n* devices, an area in the middle part of the nanowire was kept un-doped. The nanowire is covered with a 10-nm-thick SiO_2 layer. The *p*-Si substrate ($N_A \approx 1.5 \times 10^{15}$ cm^{-3}) is used as a backgate. The thickness of the buried oxide layer is 150 nm.

Devices were measured in a vacuum chamber of an electrical measurement system. *p*-type region was connected

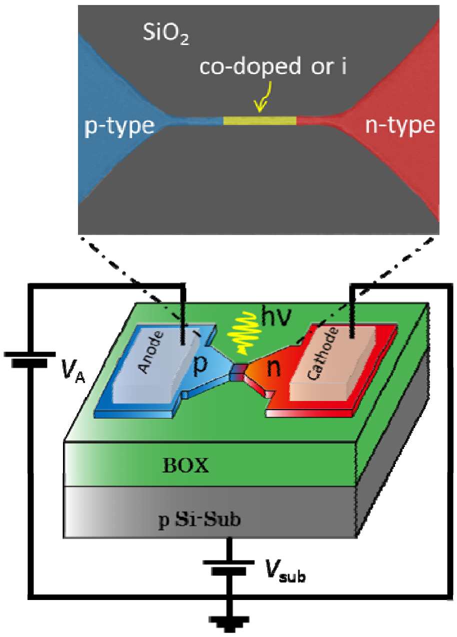

Fig. 1. Schematic device structure, bias configuration and schematic top view of *p-n* and *p-i-n* junction area.

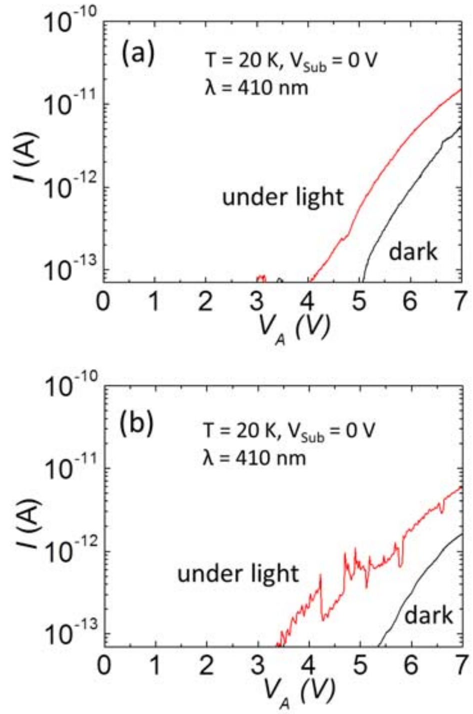

Fig. 2. Low temperature I-V_A characteristics of (a) *p-i-n* devices and (b) *p-n* junction devices. Only *p-n* junction devices show noise feature under light illumination [16].

to the voltage source, while *n*-type region and substrate were kept grounded. Light is illuminated onto the device from a halogen, light emitting diode (LED), or a monochromatic light source in the visible wavelength range. Light source is connected with optical fibers through a quartz window. The illumination area in the device has a diameter of about 3.2 mm. By dividing the measured optical power at the sample surface over the illumination area and the photon energy, the incident photon flux is estimated.

For analysis, we performed low temperature (~20 K) and room temperature measurement (~296 K). In both conditions, the devices were measured in dark and under light illumination.

III. Experimtal Results and Discussion

A. Low temperature measurement

We measured anode current versus voltage (I-V_A) characteristics at T ~ 20 K. Anode voltage was swept from negative to positive while substrate voltage (V_{sub}) was kept constant at 0 V. The main results of low temperature characteristics had been reported in our previous work [16] and will be briefly summarized in this paper. Typical I-V_A characteristics in semi logarithmic scale for *p-i-n* and *p-n* devices at low temperature are shown in Fig. 2 (a) and (b) respectively. Both devices show current enhancement under light illumination indicating that both devices are photosensitive. Although both devices show similar photosensitive behavior, it is apparent that only *p-n* junctions device show noise feature under light illumination. For further analysis, we focused on *p-n* junction devices and performed current versus time (*I-time*) measurement for fixed V_A and V_{sub} in the noisy region. In dark, current is constant, while under light illumination, current switch between two or more levels and is observed as random telegraph signal (RTS). By increasing photons intensity (Φ), we found that the number RTS increases, indicating that the RTS is triggered by photons. *I-time* characteristics in dark and under light illumination of several photon fluxes are shown in Fig. 3. As reported detail in our previous work, the noise feature is ascribed to the charging and discharging of photoexcited carrier by donor-acceptor pair in the depletion region. It is known that, at low temperature, most dopants are freeze-out [17]. The ionized donors and acceptors create a potential landscape with hills and valleys allowing electrons and holes to flow as diffusion current. The diffusion current in this device is used as a sensor to sense potential fluctuation in the channel. In dark, current is constant with time indicating no potential fluctuation. Under light illumination, photogenerated carriers can be trapped by ionized dopants causing a sudden potential change. This is sensed as anode current fluctuation (RTS) in the *I-time* characteristics. Since individual dopants basically can only accommodate a single photogenerated carrier, we suggest that, at low temperature, the nanoscale *p-n* junction devices can be utilized as single photon detectors.

B. Room temperature measurement

As low temperature characteristics have been clarified, it is important to analyze room temperature behavior for more practical application. For that purpose, we increased the temperature up to 296 K. I-V_A characteristics were measured

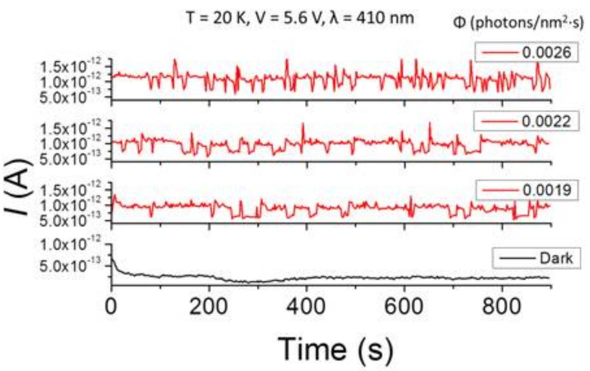

Fig. 3. *I-time* characteristics in dark and under light illumination. Under light illumination, current switch between two or more levels. By increasing incident photon flux (Φ), from bottom to up, number of RTS increases, suggesting that current jumps are triggered by photons [16].

in dark and under light illumination. Typical I-V_A characteristics in dark and under halogen light illumination for several photon fluxes (Φ) for *p-i-n* devices (a) and *p-n* devices (b) are shown in Fig. 4. Current, in absolute value, is plotted in a semi logarithmic scale; horizontal axis is applied voltage from negative (reverse) to positive (forward).

In dark, both *p-i-n* and *p-n* devices show rectifying nature which is typical characteristics of conventional diodes, i.e., current flow in forward bias and is blocked in reverse bias condition. Although both devices have different structure, *p-i-n* and *p-n* devices show identical I-V_A characteristics. Lower current in the *p-n* junction devices in the forward bias condition comes from the fact that *p-n* junction devices tend to have narrower channel size due to multiple etching processes during device fabrication. Under light illumination, both devices show photovoltaic effect, i.e., reverse current increases in negative direction by increasing photon flux (Φ), as shown in Fig. 4.

Although both devices show the same photovoltaic effect, apparently some differences can be observed. At larger forward bias condition, *p-n* junction devices show strong dependence on Φ. On the other hand, *p-i-n* junction devices show almost photon-independence. These results indicate that *p-n* junction devices are more sensitive to Φ. The origin behind this behavior most likely comes from the fact that final dimension of the *p-n* junction devices are narrower compared to *p-i-n* junction devices. This is caused by additional consumption of silicon by the double doping process in the co-doped region in *p-n* junction devices, as previously stated. The origin of the photocurrent enhancement under forward bias in *p-n* junction devices can be described as follows.

Due to narrow channel width in the *p-n* junction devices, resistance of the channel becomes high and the channel becomes insulator-like. Under bias condition, potential along the channel is tilted allowing electrons and holes to flow. Under light illumination, additional electrons and holes are generated in the channel. A small number of electrons and holes which are generated in the depletion region are immediately drifted in the opposite direction from the main

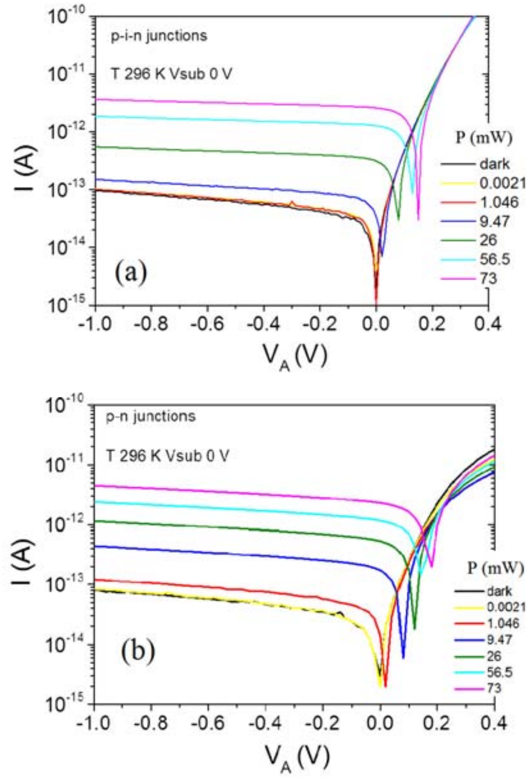

Fig. 4. Typical room temperature I-V_A characteristics of (a) *p-i-n* and (b) *p-n* junctions in dark and under light illumination. Both devices show photovoltaic effect under halogen light illumination, i.e., reverse current increases by increasing photon flux.

diffusion current. As a result, the diffusion current is slightly reduced. On the other hand, large number of photo-carriers generated in the channel beyond the depletion region is flowing in the same direction with the main diffusion current due to potential difference. This photo current increases the diffusion current.

Next, we study the effect of channel-width on device characteristics. Since both *p-i-n* and *p-n* devices show identical behavior, we focus only on the *p-n* junction devices. Fig. 5 shows typical I-V_A characteristics in dark (a) and under light illumination (b) for devices with channel length of 1000 nm and channel width varied from 275 to 1000 nm. From Fig. 5 (a), it is apparent that, in dark, current level increases by increasing channel width. These results are consistent with theoretical prediction. It is well known that dark current in *p-n* junction devices is proportional to the device area (A). Increasing the device width will eventually increase the dark current as well. Observation of reverse bias current under light illumination, however, is surprising. As shown in Fig. 5 (b), for V_A below 0 V, devices with narrow channel-width tend to have larger current enhancement under the same Φ. The trend of current enhancement for several devices with different channel width is plotted in Fig. 6.

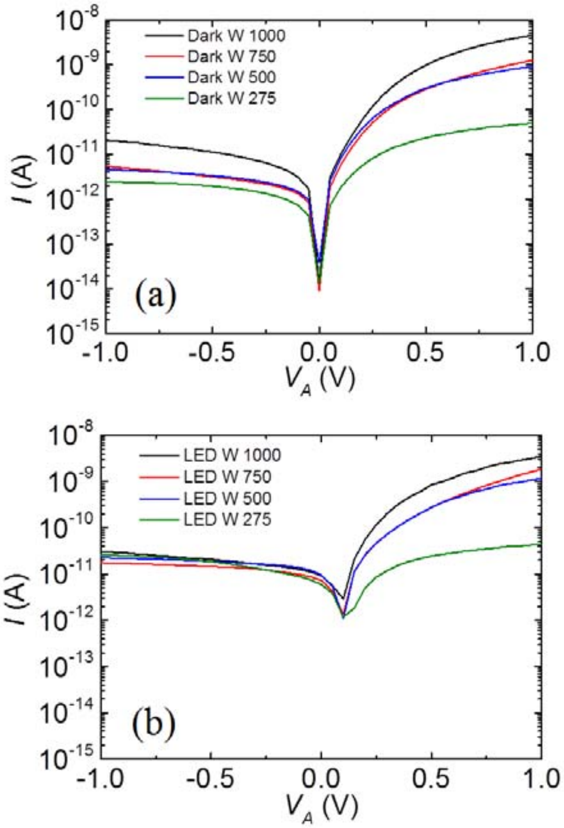

Fig. 5. I-V_A characteristics of *p-n* junction devices in (a) dark and (b) under LED illumination for several devices with different channel width. Under LED illumination, narrow channel-width devices show higher photosensitivity.

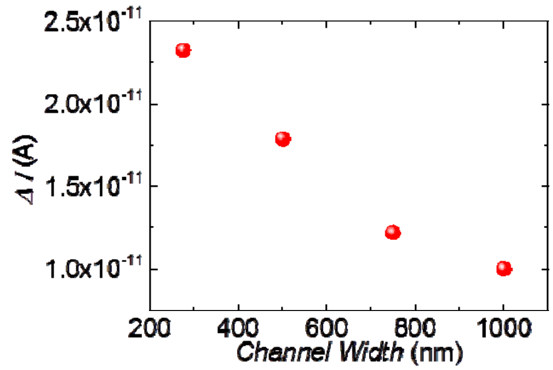

Fig. 6. Current enhancement (ΔI) due to light illumination for several devices with different channel-width. Narrow devices have larger ΔI indicating that they are generating current from photons efficiently.

As shown in Fig. 6, the current enhancement, i.e., the different current measured in dark and under light illumination, due to photovoltaic effect is larger for devices with narrow channel width. These results suggest that narrow devices are more effective in generating current under the same photon flux. Although the reason behind this trend has not been fully clarified, it is most likely that narrow devices, due to nanosize effect, have wider space-charge region as theoretically predicted by Petrosyan [18].

In conclusion, we experimentally studied nanosize effect in nanoscale lateral *p-n* and *p-i-n* junction devices at low and at room temperature. At low temperature, due to nanosize effect, individual donor-acceptor atom in *p-n* junction devices plays an important role for photon detection. At room temperature, narrow channel-width devices have larger current enhancement under light illumination. Thus, nanoscale *p-n* junction devices are promising for future photonic application.

Acknowledgment

We thank S. Miki for his support during experiment and R. Nowak for helpful discussions.

References

[1] S.M. Sze, Physics of Semiconductor Devices, 2nd ed. (John Wiley & Sons, New York, 1981), p. 63.

[2] B. Tian, X. Zheng, T.J. Kempa, Y. Fang, N. Yu, G. Yu, J. Huang, and C.M. Lieber, "Coaxial silicon nanowires as solar cells and nanoelectronic power sources.," Nature, 449, pp. 885–9, 2007.

[3] E. Garnett and P. Yang, "Light trapping in silicon nanowire solar cells.," Nano Lett., 10, pp. 1082–7, 2010.

[4] C. Yang, C.J. Barrelet, F. Capasso, and C.M. Lieber, "Single p-type/intrinsic/n-type silicon nanowires as nanoscale avalanche photodetectors.," Nano Lett., 6, pp. 2929–34, 2006.

[5] M.E. Reimer, M.P. van Kouwen, M. Barkelid, M. Hocevar, M.H.M. van Weert, R.E. Algra, E.P. a. M. Bakkers, M.T. Bjo□rk, H. Schmid, H. Riel, L.P. Kouwenhoven, and V. Zwiller, "Single photon emission and detection at the nanoscale utilizing semiconductor nanowires," J. Nanophoton., 5, p. 053502, 2011.

[6] D. Reuter, C. Werner, a. D. Wieck, and S. Petrosyan, "Depletion characteristics of two-dimensional lateral p-n-junctions," Appl. Phys. Lett., 86, p. 162110, 2005.

[7] S. Saito, D. Hisamoto, H. Shimizu, H. Hamamura, R. Tsuchiya, Y. Matsui, T. Mine, T. Arai, N. Sugii, K. Torii, S. Kimura, and T. Onai, "Electro-Luminescence from Ultra-Thin Silicon," Jpn. J. Appl. Phys., 45, pp. L679–L682, 2006.

[8] H. Sellier, G.P. Lansbergen,

[9] J. Caro, and S. Rogge, "Transport Spectroscopy of a Single Dopant in a Gated Silicon Nanowire," Phys. Rev. Lett., 97, p. 206805, 2006.

[10] Y. Ono, K. Nishiguchi, A. Fujiwara, H. Yamaguchi, H. Inokawa, and Y. Takahashi, "Conductance modulation by individual acceptors in Si nanoscale field-effect transistors," Appl. Phys. Lett., 90, p. 102106, 2007.

[11] G.P. Lansbergen, R. Rahman, C.J. Wellard, I. Woo, J. Caro, N. Collaert, S. Biesemans, G. Klimeck, L.C.L. Hollenberg, and S. Rogge, "Gate-induced quantum-confinement transition of a single dopant atom in a silicon FinFET," Nat. Phys., 4, pp. 656–661, 2008.

[12] M. Pierre, R. Wacquez, X. Jehl, M. Sanquer, M. Vinet, and O. Cueto, "Single-donor ionization energies in a nanoscale CMOS channel.," Nature nanotechnology, 5, pp. 133–7, 2010.

[13] M. Tabe, D. Moraru, M. Ligowski, M. Anwar, R. Jablonski, Y. Ono, and T. Mizuno, "Single-Electron Transport through Single Dopants in a Dopant-Rich Environment," Phys. Rev. Lett., 105, p. 016803, 2010.

[14] E. Hamid, D. Moraru, J.C. Tarido, S. Miki, T. Mizuno, and M. Tabe, "Single-electron transfer between two donors in nanoscale thin silicon-

on-insulator field-effect transistors," Appl. Phys. Lett., 97, p. 262101, 2010.

[15] E. Prati, M. Belli, S. Cocco, G. Petretto, and M. Fanciulli, "Adiabatic charge control in a single donor atom transistor," Appl. Phys. Lett., 98, p. 053109, 2011.

[16] A. Udhiarto, D. Moraru, T. Mizuno, and M. Tabe, "Trapping of a photoexcited electron by a donor in nanometer-scale phosphorus-doped silicon-on-insulator field-effect transistors," Appl. Phys. Lett., 99, p. 113108, 2011.

[17] A. Udhiarto, D. Moraru, S. Purwiyanti, Y. Kuzuya, T. Mizuno, H. Mizuta, and M. Tabe, "Photon-Induced Random Telegraph Signal Due to Potential Fluctuation of a Single Donor–Acceptor Pair in Nanoscale Si p–n Junctions," Appl. Phys. Express, 5, p. 112201, 2012.

[18] D.P. Foty, "Impurity ionization in MOSFETs at very low temperatures," Cryogenics, 30, pp. 1056–1063, 1990.

[19] A.S. Achoyan, A.É. Yesayan, É.M. Kazaryan, and S.G. Petrosyan, "Two-dimensional p-n junction under equilibrium conditions," Semiconductors, 36, pp. 903–907, 2002.